Variable Buoyancy Control for a Bottom Skimming Autonomous Underwater Vehicle

Anthony H. Sylvester III, Jeffrey A. Delmerico, A Zachary Trimble, Brian S. Bingham
Field Robotics Laboratory
University of Hawaii at Manoa
Honolulu, HI 96822
asylvest@hawaii.edu, jad4@hawaii.edu, atrimble@hawaii.edu, bsb@hawaii.edu

***Abstract*—Two feedback controllers are presented that utilize data averaging and model-based estimation to offset the effects of sensor noise and achieve precise control of an autonomous underwater vehicle (AUV) variable buoyancy system (VBS). Operation of the bottom skimming AUV requires a constant reaction force between the seabed and the vehicle. While performing a mission, variable seafloor topography and a changing payload weight requires the use of a VBS to maintain the reaction force. Two traits of the VBS system that make this a challenging problem are the presence of sensor noise and fast on/off actuation relative to the sensor update rate. It was discovered that both controllers function under these conditions but the model-based controller provides more precise control of the system. This paper presents a comparison between these two control algorithms based on both simulation results and field experiments in a coastal environment.**

Keywords—on/off actuator; variable buoyancy control; AUV; autonomous underwater vehicle; bang-bang control; noise filtering

I. INTRODUCTION

The goal of this work is to implement a variable buoyancy system (VBS) for a bottom skimming AUV that transits the sea floor while maintaining constant contact with the seabed. Furthermore the VBS should regulate the negative buoyancy of the vehicle so that the sediment exerts a constant, precise normal force on the AUV despite changes in the mass of the vehicle during a mission.

The VBS consists of a variable volume ballast chamber and a sensor to measure the normal force between the seabed and the AUV. The volume of the air-filled ballast chamber is changed by adding air from fixed volume compressed air cylinders or venting air from the chamber to seawater. This actuation of the VBS system is accomplished using two on/off solenoid valves commanded via a digital signal to be in either a fully open or fully closed state. The reaction force between the AUV and ocean floor is obtained from the output of a load cell situated to measure the net upward force provided by the ballast chamber (see Fig. 1).

A number of different approaches to variable buoyancy control have been used to successfully regulate the buoyancy of autonomous underwater vehicles (AUVs) [1]. A review of the literature shows that classic PI control, sliding mode control, and fuzzy logic control have all been applied to the

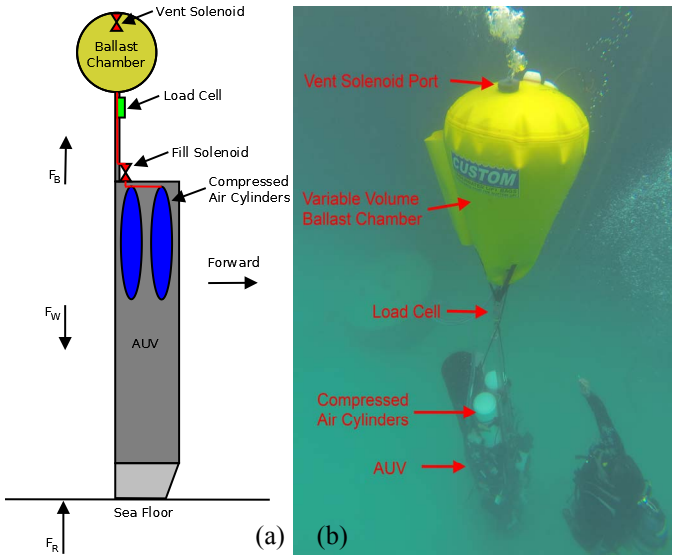

Fig. 1 a) AUV conceptual image in the X-Z plane. F_B is the buoyant force from the ballast chamber, F_W is the wet weight of the vehicle, and F_R is the reaction force between the vehicle and the sea floor. b) Venting of the VBS variable volume ballast chamber during AUV field trials in Hawaii.

control of underwater vehicle buoyancy and depth regulating systems. In [3], sliding mode control of vehicle pitch is designed to compensate for a net positive vehicle buoyancy, and actuation is provided by continuously articulated elevator fins. Riedel et al. utilize a linear-quadratic regulator in their ballast controller, which actuates ballast pumps with variable flow rate located fore and aft in their AUV to control pitch and depth, in addition to vertical thrusters [4]. In [5], DeBitetto proposes a fuzzy logic controller for an AUV with a similar mechanical arrangement to [4], utilizing variable flow rate ballast pumps. However, the reviewed buoyancy control techniques are not applicable to the binary on/off actuators in this type of system. Other work was investigated where on/off solenoids are used in controlling air ventilation [6] and teleoperated systems [7]. In [6] the on/off solenoids are controlled using PWM signals, whereas [7] makes use of sliding mode control to actuate a number of on/off solenoids in the system. Both sliding mode control and PWM control are not feasible for the as-built AUV due to existing mechanical and instrumentation limitations. These limitations will be discussed in further sections. It was therefore necessary to

978-1-4799-4918-2/14/$31.00 ©2014 IEEE

develop the moving average and model-based methods presented here. A survey of model predictive control methods is presented in [8], and the model-based controller developed in this paper is similar to the simplified Kalman filter described therein.

The VBS is implemented with feedback control to actively change the volume of the ballast chamber based on the load cell measurements. Two characteristics of the VBS make developing the feedback control system challenging. First, the analog voltage output from the load cells is highly susceptible to electromagnetic noise from nearby electric motors, despite the inclusion of twisted-shielded-pair wiring and low-pass filters. This noise is illustrated in Fig. 2. One way to address this added noise is to introduce software filtering such as a moving average filter, but this addition can introduce significant time delays in the feedback loop which can be destabilizing. Second, the rate of volume change produced by the solenoid valves is high relative to the moving average filter time delay which is a further destabilizing influence on the system. The results reported here consider the design of the VBS system as fixed and focus on implementation of feedback control algorithms capable of addressing these challenges.

II. Control Approach

The goal of this research is to implement two different estimation and control algorithms capable of addressing the challenges described above and to quantify the trade-offs between the two approaches using both computer simulation and field experiment results. The first control approach is a moving average filter coupled with a bang-bang controller and is shown in Fig. 3. The second approach is a model-based controller, comprised of a Kalman filter estimator coupled with a bang-bang controller and is shown in Fig. 4. For the remainder of the paper the model-based controller will be referred to as the Kalman filter controller. A bang-bang type controller is known alternatively as an on/off controller and is

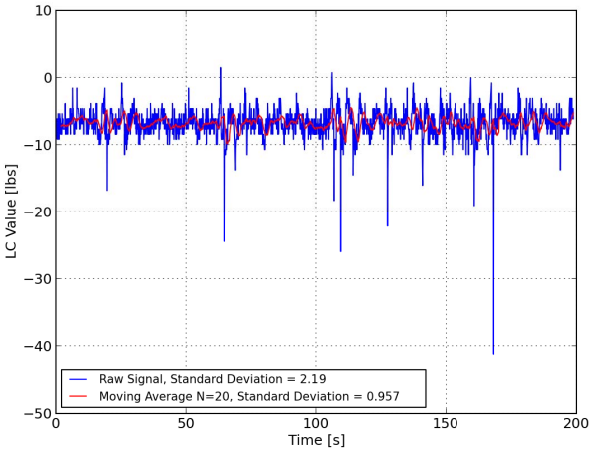

Fig. 2 Raw normal force measurements from the VBS load cell (blue) after passing through a hardware low-pass filter. It is assumed that the remainder of the noise is broadband. The true normal force is constant, but the sensor signal shows a standard deviation of ±2.19 lbs due to noise. To meet the system requirements a standard deviation of ±1 lb is necessary. The moving average (red) accomplishes this.

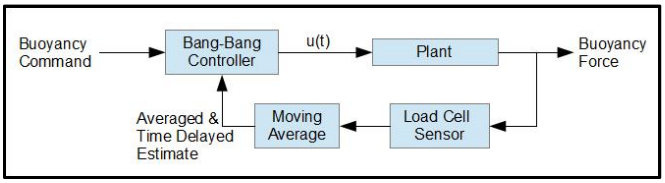

Fig. 3 Moving average bang-bang controller

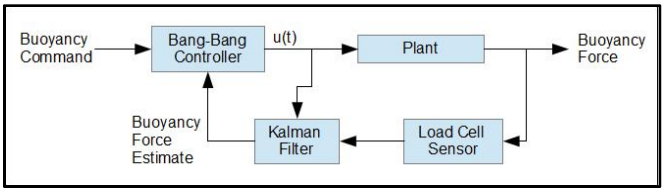

Fig. 4 Model-based Kalman filter bang-bang controller

commonly used in thermostats to control temperature. This controller method matches well with the Boolean on/off nature of the actuator solenoid valves. However, the utility of bang-bang control is limited by the size of the operational deadband. Without a deadband the bang-bang controller would switch rapidly between states when approaching the commanded setpoint. When used in a real-world environment the input values to the bang-bang controller are susceptible to noise. The presence of noise requires a large deadband for the controller to function without causing large unwanted overshoot and oscillations in response to changes in sensed buoyancy. On the AUV this noise is believed to originate from conductive coupling, as well as radiative coupling from electromagnetic motors.

A. *Moving average filter with bang-bang controller*

To address the noise in the load cell signal and decrease the size of the deadband for more precise control, a moving average filter is applied to the sensor input to estimate the true normal force. The moving average filter was applied over 20 samples. As can be seen in Fig. 2, the standard deviation of the averaged sample is decreased by 56.3% from the standard deviation of the raw data samples. However, it is expected that the standard deviation of the averaged sample would decrease by 77.6% from the raw data standard deviation based on the variance of the sample mean for a sample size of 20 units.

The use of a moving average does introduce a time delay. For the case where 20 samples are averaged with a sample frequency of 10 Hz, a significant delay of 0.95 seconds is introduced. The delay is defined as

$$Delay = \left(\frac{N-1}{2}\right) * \left(\frac{1}{f_s}\right) \quad (1)$$

where N is the number of samples and f_s is the sample frequency. Within the timescale of operations on this vehicle, a delay of 0.95 seconds is considered large.

B. *Kalman filter with bang-bang controller*

An alternative approach is to combine a Kalman filter estimator with the bang-bang controller. The Kalman filter utilizes a model of the system along with raw inputs from the sensor to output a state estimate that is closer to the true value

measured by the sensor before the unwanted addition of sensor noise. The bang-bang controller would then act on this filtered estimate as shown in Fig. 4.

III. System Model

A. VBS Model

The VBS system as illustrated in Fig. 1, is modeled based on the assumptions that air is treated as an ideal gas, and the air within the ballast chamber is both isothermal and of homogeneous temperature. A free body diagram was also generated to relate the buoyancy force due to the ballast chamber and the vehicle wet weight to determine the vehicle reaction force with the sea floor. The resulting model captures the rate of change of the system buoyancy based on the control inputs and the characteristics of the system. The model is then applied to the Kalman filter algorithm to estimate the actual buoyant force on the system resulting from the VBS.

$$F_R = F_W - F_B \tag{2}$$

$$F_W = g\left[m_A - m_V - \left(\frac{\Delta m_P}{\Delta t}\right)\right] \tag{3}$$

$$V = \frac{nRT}{P} = \frac{m}{M}\frac{RT}{P} \tag{4}$$

$$\frac{dF_B}{dt} = \rho g\left[\frac{mRT}{(M)(P)}\right]\left[q_f(u_f) - q_v(u_v)\right] \tag{5}$$

$$q_f(u_f) = \begin{cases} C_f & u_f = 1 \\ 0 & u_f = 0 \end{cases} \tag{6}$$

$$q_v(u_v) = \begin{cases} C_v & u_v = 1 \\ 0 & u_v = 0 \end{cases} \tag{7}$$

The reaction force resulting from the free body diagram is given by (2) where F_R is the reaction force, F_W is the wet weight of the vehicle, and F_B is the buoyancy force. Equations (3) and (6) can then be substituted into (2) to model the vehicles reaction force with the sea floor. The vehicle wet weight is found using (3) where m_A is the mass of the vehicle in air, m_V is the total mass of the water displaced by the vehicle, and Δm_P is the change in mass of the payload over a change in time Δt. The buoyancy force is obtained by finding the volume of the ballast chamber to determine the volume of water displaced. The volume of the ballast chamber can be determined from (4) where R is the ideal gas constant, T is the air temperature, m is the mass of air, M is the molar mass of air, and P is the ambient pressure. The volume calculated from (4) can then be substituted into (5) to obtain the change in buoyancy force with respect to time. In (5) ρ is sea water density, g is acceleration due to gravity, q_f is the mass flow rate of the fill valve, q_v is the mass flow rate of the vent valve, u_f is the fill control signal, and u_v is the vent control signal. The fill rate q_f in (6) is dependent upon u_f the fill control signal, similarly the vent rate q_v in (7) is dependent upon the vent control signal u_v. The fill and vent control signals u_f and u_v can only exist as on/off corresponding to a numeric value of 1 or 0. When u_f is equal to 1 then q_f is equal to the constant fill rate C_f and when u_v is equal to 1 then q_v is equal to a constant vent rate C_v. Both fill and vent rates C_f and C_v respectively are dependent upon the ambient pressure and the compressed air supply pressure. For this exercise the fill and vent rates were experimentally determined at a fixed depth.

For this study it is assumed the air flow rates of the system are constant when the solenoid valves are in their open state. Field trials are currently only conducted at a constant water depth of 20 ft. therefore as the depth increases the effects on the VBS due to increased pressure are neglected. This is an area that will be investigated further during future work on this project.

B. Kalman filter model

The Kalman filter controller was developed from a simplified version of the discrete Kalman filter. For controlling the VBS it was only necessary to estimate one value, the buoyant force. This resulted in a version of the filter where some of the matrices are reduced to scalar values. The simplified equations used are presented below.

$$X_{P[k+1]} = X_{E[k]} + \left[C_f(dt)\ C_v(dt)\right]\left[u_{f[k]};\ u_{v[k]}\right] \tag{8}$$

$$K_{[k+1]} = \frac{P_{E[k]}+q}{P_{E[k]}+q+r} \tag{9}$$

$$P_{E[k+1]} = \left(P_{E[k]} + q\right) - K_{[k+1]}\left(P_{E[k]} + q\right) \tag{10}$$

$$X_{E[k+1]} = X_{P[k+1]} + K_{[k+1]}\left(Z_{[k+1]} - X_{P[k+1]}\right) \tag{11}$$

The predicted state is represented as $X_{P[k+1]}$ in (8), where $X_{E[k]}$ is the previous state estimate, C_f is the air fill flow rate, C_v is the air vent rate, $u_{f[k]}$ is the fill control input, and $u_{f[k]}$ is the vent control input. The Kalman gain $K_{[k+1]}$ is updated using (9) where $P_{E[k]}$ is the previous covariance estimate, q is the process noise, and r is the measurement noise. The state covariance is updated in (10). An updated state estimate is then achieved from (11) where the predicted state estimate $X_{P[k+1]}$ is summed with the product of the Kalman gain $K_{[k+1]}$ from (9) and the difference of the new sensor measurement $Z_{[k+1]}$ and the previous predicted state $X_{P[k+1]}$. This process is repeated for each new measurement and control input received, and then returns updated values for the state estimate and state estimate covariance.

IV. Results and Discussion

A series of experiments were performed to validate and compare the two control approaches, first in a computer simulation environment, then in the field with both controllers deployed on the AUV.

A. Simulation results

To compare and contrast the two filters a square wave was generated using zero mean, additive, Gaussian white noise with a standard deviation of 2.19 lbs (see Fig. 2) in order to simulate the random errors evident in the load cell measurements. This square wave is then processed through both filters to test their functionality and ability to produce a state estimate from a noisy signal. The response of both filters to this simulation is shown in Fig. 5 and Fig. 6, where the generated noise on the square wave is consistent with the measured noise from Fig. 2.

A second simulation test was performed using actual experimental data in order to observe the behavior of the moving average and Kalman filter estimates. Log files from previous experiments included both the raw load cell measurements and the solenoid valve commands. These log files were recorded using the lightweight communications and

marshalling (LCM) library [9]. The LCM library includes a player to allow the log file to be broadcast to the network. This functionality was used to evaluate the two filters prior to implementing the controllers. The log file was played back in real time and both the moving average filter and Kalman filter were executed and produced estimates of the state of the load cell. This is shown in Fig. 7 and Fig. 8. While the noise on the load cell sensor had been previously characterized in Fig. 2, it is noted that the logged data used in Figs. 7 and 8 appears to have a higher noise standard deviation. This higher presence of noise could be the result of different ocean conditions than during previous tests. Despite the added noise, both filters were tested with the logged data and found to be functional.

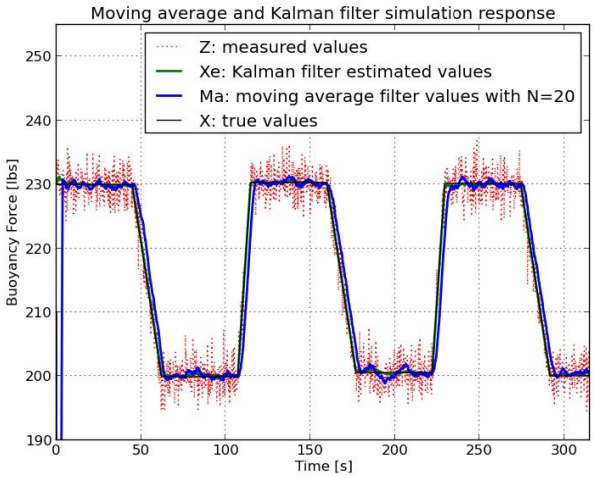

Fig. 5 Moving average filter and Kalman filter tested in simulation. The measured values Z were generated using the true values X and zero mean, additive, Gaussian white noise with a standard deviation of 2.19 lbs. Note the delay in the moving average filter estimates (blue).

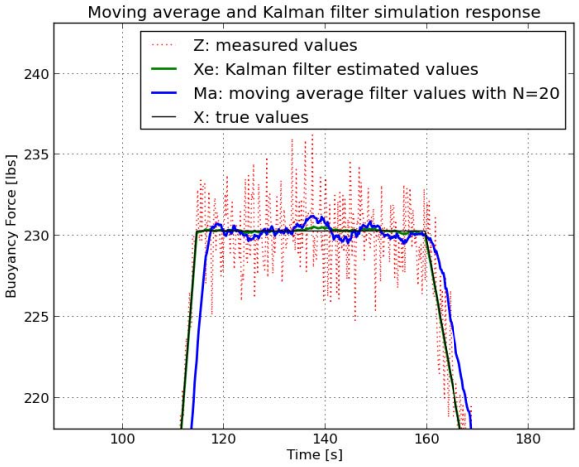

Fig. 6 Close up view of the filter estimates for one step input, taken from (Fig. 5). The time delay on the moving average estimate is easily viewed on the rising and falling slopes of the step response.

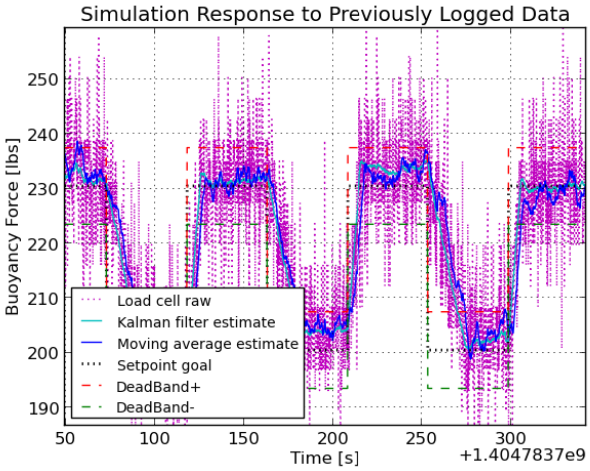

Fig. 7 Moving average filter and Kalman filter response tested in simulation using previously logged data from the AUV load cell

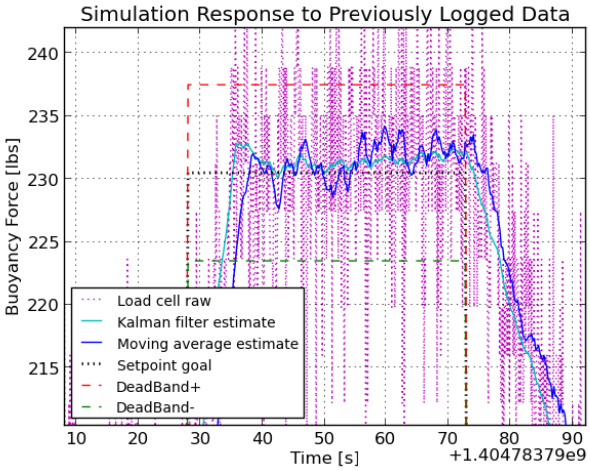

Fig. 8 Close up view of one step input response, taken from (Fig. 7). The Kalman filter estimate (cyan) produces a state estimate ahead of the moving average estimate (blue) and with smaller oscillations about the setpoint value.

1) Moving average filter with bang-bang controller

The moving average filter was able to produce a state estimate with a much smaller standard deviation than the simulated raw data. However, the inherent time delay resulting from the moving average filter is present and appeared consistent with the predicted time delay of 0.95 seconds for a moving average calculated over a series of 20 samples, this behavior is visible in Fig. 6 which provides a close up view of one step input taken from Fig. 5. The moving average filter response is identified as the blue colored data set in Fig. 5, the Kalman filter response is represented as the green data set, the raw data as red, and the true values are represented by the black colored data set.

2) Kalman filter with bang-bang controller

The Kalman filter developed for controlling the VBS was first tuned in the simulator environment. The measurement noise r was identified based on the measured variance of the

load cell as illustrated in Fig 2 where $\sigma = 2.19$ lbs and $r = \sigma^2 = 4.80$ lbs^2. With r held constant, the process noise q was varied from $0.0 \leq q \leq r$ until a desirable response was achieved. A process noise value of $q = 0.001$ lbs^2 was used for this system.

It can be seen in Fig. 5 and Fig. 6 that the Kalman filter state estimate conforms closely to the true values in the open loop simulation. The simulated Kalman filter response is more desirable than the moving average filter response due to increased accuracy and the absence of the time delay. This behavior was also observed in the second set of simulation tests conducted where a previous log of the load cell output was played back during a step response mission. In Fig. 7 and Fig. 8 it can be observed that the Kalman filter estimator (cyan) produces a more consistent state prediction than the moving

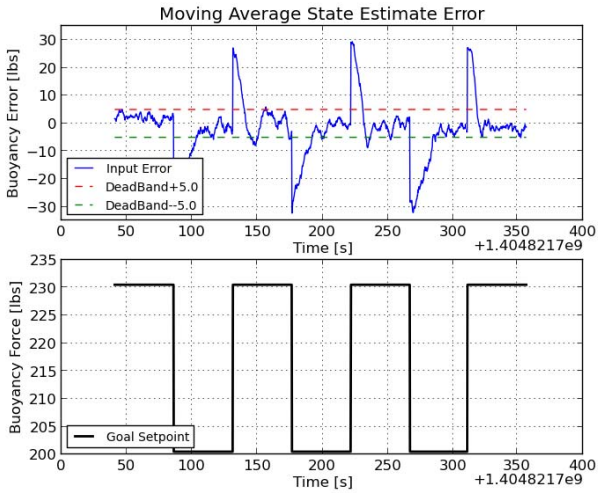

Fig. 9 State estimation error in response to a step input with a bang-bang controller deadband of +/- 5 lbs. This deadband appears to be the operational limit of the moving average filter estimator.

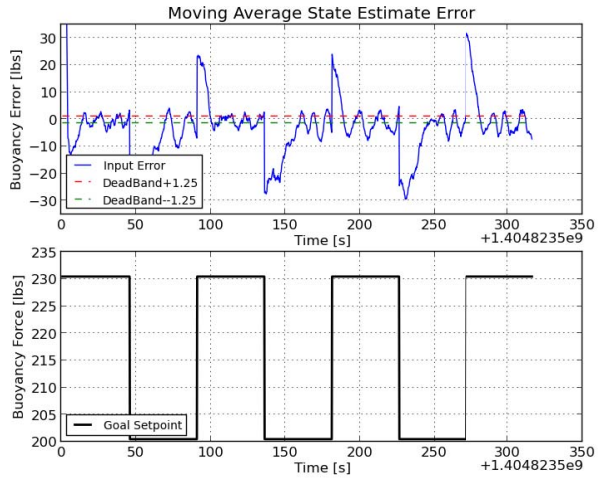

Fig. 10 State estimation error for a deadband of +/- 1.25 lbs. The moving average controller is unstable at this point with the presence of obvious oscillations and continual overshoot beyond the deadband bounds. This would result in rapid cycling of the solenoid valves and likely lead to their failure. Additionally the system is unable to achieve a steady state buoyancy.

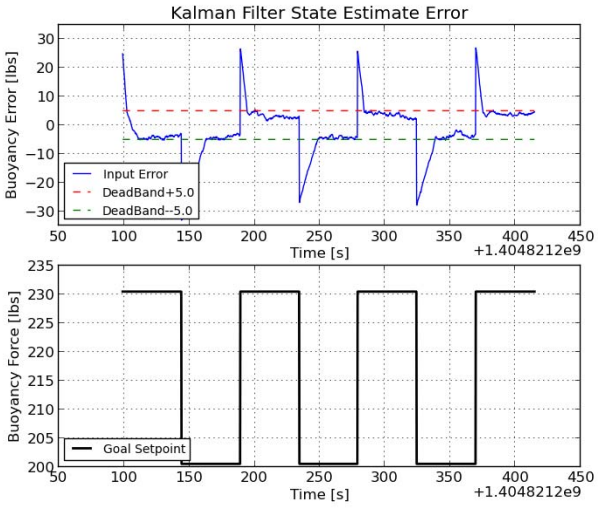

Fig. 11 The Kalman filter estimator responds well to a step input with a deadband of +/- 5 lbs. Once the controlled response reaches a deadband it does not overshoot.

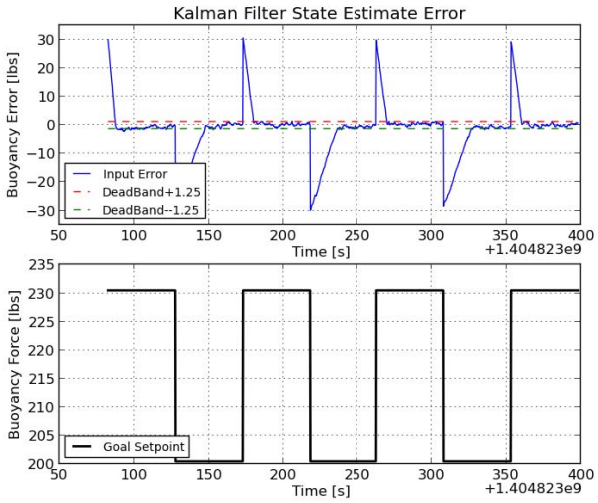

Fig. 12 Kalman filter state estimation response with a control deadband of +/- 1.25 lbs. The filter performs well at this range with no overshoot and quick conversion to a minimal amount of state error. At this range the Kalman filter estimator clearly outperforms the moving average filter.

average response (blue) despite the large amount of sensor noise in the raw data (magenta).

B. Experimental results

Upon obtaining satisfactory results from both filters in simulation, a series of field tests were conducted. For the tests, the vehicle was situated at a depth of 20 ft. below sea level. The AUV was stationary, and the test site is located in an area protected from direct ocean waves.

The AUV was programmed to perform step responses in buoyancy setpoint value represented by a 30lb amplitude square wave over 315 seconds (Figs. 9-12). This experiment was then repeated with bang-bang controller deadband values

of +/- 7 lbs, +/- 5 lbs, +/- 2.5 lbs, and +/- 1.25 lbs and for each filter running active VBS feedback control. The deadbands of +/- 5 lbs and +/- 1.25 lbs were selected for plotting as they appeared to capture the operating limits of the moving average filter and the Kalman filter respectively. In general, a smaller deadband value results in more precise control of the VBS. In Figs. 9-12 the error (blue) is calculated between the buoyancy force estimate and the buoyancy force setpoint. The error is then plotted where the spikes in error (blue) occur as the setpoint is switched corresponding to the setpoint (black) in the bottom subplot of each figure.

1) Moving average filter with bang-bang controller

It was determined that the smallest deadband the moving average filter would tolerate is +/- 5 lbs from the buoyancy setpoint. This is shown in Fig. 9 where there are some small noticeable oscillations in the state response, but the state estimate error still remains within the operational deadband. This behavior is not continuous for smaller deadband sizes as can be seen in Fig. 10 where the deadband is set to +/- 1.25 lbs. The moving average state estimate error continuously overshoots the setpoint resulting in unwanted oscillations. This type of behavior is not only destabilizing for the vehicle but also taxing on the solenoid valves as they are working to rapidly open and close. The rapid actuation of the fill and vent solenoids can also lead to gas burn. The compressed air cylinders contain enough air gas to complete a mission. Constant adjustment to the ballast chamber will result in wasted gas and premature expenditure of the compressed air cylinders.

2) Kalman filter with bang-bang controller

With a deadband of +/- 5 lbs in Fig. 11, the Kalman filter state estimate error converged quickly to each deadband with little overshoot. This behavior is encouraging and suggests that the model-based controller can operate under smaller deadband conditions. The deadband was then reduced further in Fig. 12. With the deadband decreased to +/- 1.25 lbs, the state estimate error was still able to converge quickly to the bounds of the deadband and produce little to no oscillations and overshoot. The error between the buoyancy force estimate and buoyancy force setpoint quickly approaches zero in Fig. 12 suggesting that the actual vehicle buoyancy response is true to the commanded buoyancy. This result confirms that the model-based Kalman filter estimator controller can achieve more precise control of the VBS than the moving average controller, with a faster response. The Kalman filter controller was able to maintain stability beyond the operating limits of the moving average controller during actual field trials.

V. Conclusions

Preliminary experimental results show that the moving average bang-bang controller approach is operational, but the performance and stability is limited. The model-based Kalman filter control algorithm delivers more precise regulation of the VBS, faster response to un-modeled disturbances and guaranteed stability. The Kalman filter controller allows smaller deadbands for the on/off actuation thus resulting in a more predictable VBS response and state estimates that are true to the actual vehicle state. The moving average controller was only able to achieve +/- 5 lbs regulation of the VBS while the Kalman filter controller was able to achieve +/- 1.25 lbs regulation.

While this approach is developed specifically for the challenges of the VBS of a bottom skimming AUV, the same control algorithm can be used to improve the performance of any system with noisy sensor inputs and fast on/off actuation.

Acknowledgment

The authors would like to thank Makai Ocean Engineering for their involvement, resources, and support in conducting field trials and experiments.

References

[1] H. F. Jensen III, “Variable Buoyancy System Metric,” Master's Thesis, Joint Program in Applied Ocean Science and Engineering, Massachusetts Institute of Technology Dept. of Mechanical Engineering, Woods Hole Oceanographic Institute, 2009.

[2] S. Tangirala and J. Dzielski, “A Variable Buoyancy Control System for a Large AUV,” IEEE Journal of Oceanic Engineering, vol. 32, no. 4, pp. 762–771, 2007.

[3] E. Y. Hong, H. G. Soon, M. Chitre, “Depth Control of an Autonomous Underwater Vehicle, STARFISH,” Proceedings of the IEEE OCEANS Conference, Sydney, pp. 1–6, May 2010.

[4] J. Riedel, A. Healey, D. Marco, and B. Beyazay, “Design and Development of Low Cost Variable Buoyancy System for the Soft Grounding of Autonomous Underwater Vehicles,” International Symposium on Unmanned Untethered Submersible Technology; 11th, pp.427-438, 2005.

[5] P. DeBitetto, "Fuzzy logic for Depth Control of Unmanned Undersea Vehicles," AUV '94., Proceedings of the 1994 Symposium on Autonomous Underwater Vehicle Technology, pp. 233-241, 1994.

[6] I. Sardellitti, S. Cecchini, S. Silvestri, D.G. Caldwell, "Proportional mechanical ventilation through PWM driven on/off solenoid valve," Engineering in Medicine and Biology Society (EMBC), 2010 Annual International Conference of the IEEE, pp.1222-1225, 2010.

[7] M.Q. Le, M. T. Pham, M. Tavakoli, R. Moreau, "Sliding mode control of a pneumatic haptic teleoperation system with on/off solenoid valves," Robotics and Automation (ICRA), 2011 IEEE International Conference on , pp.874-879, 2011.

[8] S. J. Qin, T. A. Badgwell, “A survey of industrial model predictive control technology,” Control Engineering Practice, vol. 11, no. 7, pp.733-764, 2003.

[9] A. S. Huang, E. Olson, D. C. Moore, “LCM: Lightweight Communications and Marshalling,” Intelligent Robots and Systems (IROS), 2010 IEEE/RSJ International Conference on, pp.4057,4062, 2010.